J|A|C|S ARTICLES

Published on Web 06/19/2009

Detection of Bacterial Spores with Lanthanide−Macrocycle Binary Complexes

Morgan L. Cable,[†,‡] James P. Kirby,[*,‡] Dana J. Levine,[†,‡] Micah J. Manary,[†,‡] Harry B. Gray,[*,†] and Adrian Ponce[*,†,‡]

Beckman Institute, California Institute of Technology, Pasadena, California 91125, and Planetary Science Section, Jet Propulsion Laboratory, 4800 Oak Grove Drive, Pasadena, California 91109

Received March 28, 2009; E-mail: james.p.kirby@jpl.nasa.gov; ponce@caltech.edu; hbgray@caltech.edu

Abstract: The detection of bacterial spores *via* dipicolinate-triggered lanthanide luminescence has been improved in terms of detection limit, stability, and susceptibility to interferents by use of lanthanide−macrocycle binary complexes. Specifically, we compared the effectiveness of Sm, Eu, Tb, and Dy complexes with the macrocycle 1,4,7,10-tetraazacyclododecane-1,7-diacetate (DO2A) to the corresponding lanthanide aquo ions. The $Ln(DO2A)^+$ binary complexes bind dipicolinic acid (DPA), a major constituent of bacterial spores, with greater affinity and demonstrate significant improvement in bacterial spore detection. Of the four luminescent lanthanides studied, the terbium complex exhibits the greatest dipicolinate binding affinity (100-fold greater than Tb^{3+} alone, and 10-fold greater than other $Ln(DO2A)^+$ complexes) and highest quantum yield. Moreover, the inclusion of DO2A extends the pH range over which Tb−DPA coordination is stable, reduces the interference of calcium ions nearly 5-fold, and mitigates phosphate interference 1000-fold compared to free terbium alone. In addition, detection of *Bacillus atrophaeus* bacterial spores was improved by the use of $Tb(DO2A)^+$, yielding a 3-fold increase in the signal-to-noise ratio over Tb^{3+}. Out of the eight cases investigated, the $Tb(DO2A)^+$ binary complex is best for the detection of bacterial spores.

1. Introduction

Bacterial spores (i.e., endospores) are dormant microbial forms that exhibit remarkable resistance to chemical and physical environmental stresses.[1−3] Because they are so resilient to most sterilization procedures, bacterial spores are used in several industries as biological indicators.[4,5] As these organisms are tough enough to survive even the extreme pressures, temperatures, and radiation of space,[6] they are also the focus of research concerning panspermia and life in extreme environments.[7−9] In addition, detection of endospores became a national priority after the anthrax attacks of 2001, as *Bacillus anthracis* spore powders are the vectors of the anthrax bioweapon.[10−13] Rapid detection of dipicolinic acid (DPA), a unique chemical marker and major constituent of bacterial spores,[14] is accomplished using DPA-sensitized lanthanide luminescence under UV excitation. Enhancement of Tb^{3+} emission through an absorbance-energy transfer-emission (AETE) effect upon DPA coordination yields an increase in intensity by more than 3 orders of magnitude.[15−20] On average, DPA constitutes 10% of a bacterial spore's dry weight (10^8 molecules of DPA per spore); the luminescence intensity of the $Tb(DPA)\cdot 6H_2O$ complex can therefore be correlated to approximate spore concentration. This technique can be easily miniaturized and automated for rapid detection of a spore event[21] or possibly traces of life in extreme environments.

Although the method is rapid and straightforward, we aim to improve the Tb−DPA assay for detection of bacterial spores

[†] California Institute of Technology.
[‡] Jet Propulsion Laboratory.

(1) Bisset, K. A. *Nature* **1950**, *166*, 431–432.
(2) Driks, A. *Proc. Natl. Acad. Sci. U.S.A* **2003**, *100*, 3007–3009.
(3) Nicholson, W. L.; Munakata, N.; Horneck, G.; Melosh, H. J.; Setlow, P. *Microbiol. Mol. Biol. Rev.* **2000**, *64*, 548–572.
(4) Albert, H.; Davies, D. J. G.; Woodson, L. P.; Soper, C. J. *J. Appl. Microbiol.* **1998**, *85*, 865–874.
(5) Yung, P. T.; Ponce, A. *Appl. Environ. Microbiol.* **2008**, *74*, 7669–7674.
(6) Horneck, G.; Bucker, H.; Reitz, G. *Adv. Space Res.* **1994**, *14*, 41–45.
(7) Yung, P. T.; Shafaat, H. S.; Connon, S. A.; Ponce, A. *FEMS Microbiol. Ecol.* **2007**, *59*, 300–306.
(8) Shafaat, H. S.; Ponce, A. *Appl. Environ. Microbiol.* **2006**, *72*, 6808–6814.
(9) Nicholson, W. L. *Orig. Life Evol. Biosph.* **2003**, *33*, 621–631.
(10) Jernigan, J. A.; Stephens, D. S.; Ashford, D. A.; Omenaca, C.; Topiel, M. S.; Galbraith, M.; Tapper, M.; Fisk, T. L.; Zaki, S.; Popovic, T.; Meyer, R. F.; Quinn, C. P.; Harper, S. A.; Fridkin, S. K.; Sejvar, J. J.; Sephard, C. W. *Emerg. Infect. Dis.* **2001**, *7*, 933–944.
(11) Sanderson, W. T.; Stoddard, R. R.; Echt, A. S.; Piacitelli, C. A.; Kim, D.; Horan, J.; Davies, M. M.; McCleery, R. E.; Muller, P.; Schnorr, T. M.; Ward, E. M.; Hales, T. R. *J. Appl. Microbiol.* **2004**, *96*, 1048–1056.
(12) Yung, P. T.; Lester, E. D.; Bearman, G.; Ponce, A. *Biotechnol. Bioeng.* **2007**, *84*, 864–871.
(13) Sharp, R. J.; Roberts, A. G. *J. Chem. Technol. Biotechnol.* **2006**, *81*, 1612–1625.
(14) Murrell, W. G. *The Bacterial Spore*; Academic Press: New York, 1969.
(15) Horrocks, W. D., Jr; Sudnick, D. R. *Acc. Chem. Res.* **1981**, *14*, 384–392.
(16) Horrocks, W. D., Jr; Albin, M. *Prog. Inorg. Chem.* **1984**, *31*, 1–104.
(17) Balzani, V. *Pure Appl. Chem.* **1990**, *62*, 1099–1102.
(18) Balzani, V.; Decola, L.; Prodi, L.; Scandola, F. *Pure Appl. Chem.* **1990**, *62*, 1457–1466.
(19) Hindle, A. A.; Hall, E. A. H. *Analyst* **1999**, *124*, 1599–1604.
(20) Lehn, J. M. *Angew. Chem., Int. Ed. Engl.* **1988**, *27*, 89–112.
(21) Lester, E. D.; Bearman, G.; Ponce, A. *IEEE Eng. Med. Biol. Mag.* **2004**, *23*, 130–135.

 10.1021/ja902291v CCC: $40.75

and expand our understanding of the chemistry underpinning this sensor system. The potential for false positives or false negatives through complexation of anionic interferents to the trivalent terbium cation is a serious concern when the method is applied to environmental samples. Previous studies indicate that phosphate in particular can inhibit DPA binding or decrease luminescence intensity.[22,23] Further, coordinated water molecules can quench Tb^{3+} luminescence by nearly an order of magnitude, due to nonradiative deactivation from vibronic coupling of the OH oscillators with the excited lanthanide.[24] To eliminate water from the Tb^{3+}-coordination sphere and reduce the potential for interfering ion effects, we have introduced a macrocyclic ligand, DO2A (1,4,7,10-tetraazacyclododecane-1,7-diacetate), to form a first generation DPA receptor site. DO2A meets our initial conditions for a receptor site ligand, in that it binds strongly to Tb^{3+} (log $K_{GdDO2A} = 19.42$[25]) without impeding DPA binding. Our previous work using a binding affinity by competition (BAC) assay[26] demonstrates a 2 order of magnitude increase in the DPA binding affinity with the $Tb(DO2A)^+$ binary complex over the Tb^{3+} aquo species.[27]

The extraordinary stability of the $Tb(DO2A)(DPA)^-$ complex has improved lanthanide-based detection of dipicolinate under optimal conditions. However, detection of bacterial spores in an environmental context will require receptor sites that are resistant to variations in pH and temperature, in addition to competing ion effects.

Here, we present characterization of four luminescent $Ln(DO2A)(DPA)^-$ ternary complexes (Ln = Sm, Eu, Tb and Dy) to probe structural effects on the enhanced stability induced by DO2A; we also examine the stability of these complexes as a function of temperature, pH, and competitive ion concentrations. The dipicolinate sensor complex that exhibits the highest stability and effective discrimination against competitive ion binding was then tested using real bacterial spores.

2. Experimental Section

2.1. Materials. The following chemicals were purchased and used as received: ammonium chloride (J.T. Baker), calcium chloride trihydrate (Aldrich), CAPS (*N*-cyclohexyl-3-aminopropanesulfonic acid) buffer (Alfa Aesar), cesium chloride (MP Biomedicals), CHES (*N*-cyclohexyl-2-aminoethanesulfonic acid) buffer (Alfa Aesar), DPA (dipicolinic acid, pyridine-2,6-dicarboxylic acid) (Aldrich), dysprosium(III) chloride hydrate (Alfa Aesar), europium(III) chloride hexahydrate (Aldrich), lithium chloride (Aldrich), magnesium chloride hexahydrate (Mallinckrodt), MES monohydrate (2-(*N*-morpholino)ethanesulfonic acid monohydrate) buffer (Alfa Aesar), MOPS (3-(*N*-morpholino)-propanesulfonic acid) buffer (Alfa Aesar), potassium chloride (Mallinckrodt), samarium(III) chloride (Alfa Aesar), sodium acetate trihydrate (Mallinckrodt), sodium bromide (J.T. Baker), sodium carbonate (Mallinckrodt), sodium chloride (EM Science), sodium citrate dihydrate (Mallinckrodt), sodium fluoride (Aldrich), sodium hydroxide (NaOH 50% in water) (Mallinckrodt), sodium iodide hydrate (Alfa Aesar), sodium nitrate (Mallinckrodt), sodium phosphate tribasic dodecahydrate (BDH), anhydrous sodium sulfate (Mallinckrodt), TAPS (*N*-tris(hydroxymethyl)methyl-3-aminopropanesulfonic acid) buffer (TCI America), terbium(III) chloride hexahydrate (Alfa Aesar), tetrabutylammonium hydroxide (TBAOH 10% in 2-propanol) (TCI America) and L-tryptophan (Alfa Aesar). All lanthanide salts were 99.9% pure or greater, all other salts were 99% pure or greater, and all buffers were at least 98% pure. Water was deionized to a resistivity of 18.2 MΩ-cm using a Siemens Purelab Ultra laboratory water purification system. The 1,4,7,10-tetraazacyclododecane-1,7-diacetate (DO2A) ligand was prepared by hydrolysis of 1,4,7,10-tetraazacyclododecane-1,7-di(*tert*-butyl acetate) (Macrocyclics), as described previously[27] resulting in a white solid in 99.8% yield. $DO2A \cdot 2.80HCl \cdot 0.85H_2O$. Anal. Calcd (found) for $C_{12}H_{24}N_4O_4 \cdot 2.80HCl \cdot 0.85H_2O$ (fw = 405.57): C, 35.54 (35.54); H, 7.08 (6.72); N, 13.81 (13.25); Cl, 24.43 (25.10). *Bacillus atrophaeus* bacterial spores (ATCC 9372) were purchased from Raven Biological Laboratories and stored at 4 °C until use.

2.1.1. Synthesis of Lanthanide Complexes. The procedure to generate the $Ln(DO2A)(DPA)^-$ ternary complex (Ln = Sm, Eu, Tb, Dy) as a tetrabutylammonium (TBA) salt has been described previously for the Tb and Eu species[26,27] and is similar for the analogous Sm and Dy complexes. Slow crystallization from acetone yielded clear colorless (Eu, Tb, Dy) or yellow (Sm) crystals suitable for X-ray diffraction. **TBA·Sm(DO2A)(DPA)**. 0.474 g, yield: 44.8%. Anal. Calcd (found) in duplicate for $NC_{16}H_{36} \cdot SmC_{19}H_{25}N_5O_8 \cdot 3.29H_2O \cdot 0.21C_{16}H_{36}NCl$ (fw = 960.8): C, 47.88 (47.80); H, 7.87 (7.40); N, 9.05 (9.32); Sm, 15.65 (15.65). ESI-MS (*m*/*z*): calcd (found) for $SmC_{19}H_{25}N_5O_8$ (M^-) 603.4 (603.1). **TBA·Eu(DO2A)(DPA)**. 0.269 g, yield: 38.9%. Anal. Calcd (found) in duplicate for $NC_{16}H_{36} \cdot EuC_{19}H_{25}N_5O_8 \cdot 3.52H_2O \cdot 0.93C_{16}H_{36}NCl$ (fw = 1168.8): C, 51.32 (51.33); H, 8.77 (8.00); N, 8.31 (8.49); Eu, 13.00 (12.95). ESI-MS (*m*/*z*): calcd (found) for $EuC_{19}H_{25}N_5O_8$ (M^-) 604.4 (604.1). **TBA·Tb(DO2A)(DPA)**. 0.301 g, yield: 42.3%. Anal. Calcd (found) in duplicate for $NC_{16}H_{36} \cdot TbC_{19}H_{25}N_5O_8 \cdot 1.00C_3H_6O \cdot 4.00H_2O$ (fw = 982.97): C, 46.43 (46.63); H, 7.69 (8.17); N, 8.55 (8.71); Tb, 16.17 (15.65). ESI-MS (*m*/*z*): calcd (found) for $TbC_{19}H_{25}N_5O_8$ (M^-) 610.4 (610.1). **TBA·Dy(DO2A)(DPA)**. 0.102 g, yield: 45.4%. Anal. Calcd (found) in duplicate for $NC_{16}H_{36} \cdot DyC_{19}H_{25}N_5O_8 \cdot 9.24H_2O \cdot 1.45C_{16}H_{36}NCl$ (fw = 1426.9): C, 49.04 (49.05); H, 9.31 (7.66); N, 7.32 (8.68); Dy, 11.39 (11.40). ESI-MS (*m*/*z*): calcd (found) for $Dy_1C_{19}H_{25}N_5O_8$ (M^-) 615.4 (615.1).

2.2. Methods. Unless otherwise specified, all samples were prepared in triplicate to a final volume of 4.00 mL in disposable acrylate cuvettes (Spectrocell), 1 cm path length, and were allowed to equilibrate for at least 24 h before analysis using a Fluorolog-3 Fluorescence Spectrometer (Horiba Jobin-Yvon) at 25 °C. To prevent the second-order diffraction of the source radiation, a 350-nm colorless sharp cutoff glass filter (Melles Griot 03 FCG 055) was used in all measurements. All reported spectra were obtained as a ratio of corrected signal to corrected reference (S_c/R_c) to eliminate the effect of varying background radiation in the sample chamber; emission intensities are in units of counts per second per microampere (cps/μA).

2.2.1. X-ray Crystallography. The crystal structures of TBA·Tb(DO2A)(DPA) and TBA·Eu(DO2A)(DPA) were described in previous work.[26,27] Diffraction data for the Sm and Dy complexes (Table 1) were collected at 100 ± 2 K on a Bruker SMART 1000 CCD area detector diffractometer equipped with graphite monochromated Mo Kα radiation ($\lambda\alpha = 0.710\ 73$ Å). The structures were solved by isomorphous methods for $Dy(DO2A)(DPA)^-$ and direct methods for $Sm(DO2A)(DPA)^-$ and refined by full-matrix least-squares calculations on F^2 (SHELXL-97, Sheldrick, 1997). Non-hydrogen atoms were refined anisotropically. The hydrogen atoms were introduced in calculated positions. CCDC reference numbers are 643596 and 655647.

(22) Jones, G.; Vullev, V. I. *J. Phys. Chem. A* **2002**, *106*, 8213–8222.
(23) Pellegrino, P. M.; Fell, N. F.; Rosen, D. L.; Gillespie, J. B. *Anal. Chem.* **1998**, *70*, 1755–1760.
(24) Kropp, J. L.; Windsor, M. W. *J. Phys. Chem.* **1967**, *71*, 477–482.
(25) Kim, W. D.; Hrncir, D. C.; Kiefer, G. E.; Sherry, A. D. *Inorg. Chem.* **1995**, *34*, 2225–2232.
(26) Kirby, J. P.; Cable, M. L.; Levine, D. J.; Gray, H. B.; Ponce, A. *Anal. Chem.* **2008**, *80*, 5750–5754.
(27) Cable, M. L.; Kirby, J. P.; Sorasaenee, K.; Gray, H. B.; Ponce, A. *J. Am. Chem. Soc.* **2007**, *129*, 1474–1475.
(28) Nogrady, T.; Weaver, D. F. *Medicinal Chemistry: A Molecular and Biochemical Approach*; Oxford University Press: 2005; pp 67−105.

Table 1. Crystallographic Data for the Four TBA·Ln(DO2A)(DPA) Structures

Ln	Tb[a]	Eu[b]	Dy	Sm
formula	$[C_{19}H_{25}N_5O_8Tb]^-$ $[C_{16}H_{36}N]^+$ $0.47(C_3H_8O)$ $0.53(C_3H_6O)$ $3(H_2O)$	$[C_{19}H_{25}N_5O_8Eu]^-$ $[C_{16}H_{36}N]^+$ $0.68(C_3H_8O)$ $0.32(C_3H_6O)$ $3(H_2O)$	$[C_{19}H_{25}N_5O_8Dy]^-$ $[C_{16}H_{36}N]^+$ $2(C_3H_8O)$ $3(H_2O)$	$[C_{19}H_{25}N_5O_8Sm]^-$ $[C_{16}H_{36}N]^+$ $0.27(C_2H_6O\cdot O)$ $0.73(C_3H_6O)$ $2(H_2O)$
M_w	964.94	957.23	966.51	939.36
crystal system	monoclinic	triclinic	monoclinic	monoclinic
space group	$P2_1/c$	$P1$	$P2_1/c$	$P2_1/c$
a (Å)	13.1047(5)	13.1473(4)	13.1742(4)	13.0658(4)
b (Å)	13.3397(5)	13.2269(4)	13.1860(4)	13.4504(4)
c (Å)	26.0901(9)	26.2248(8)	26.1130(8)	26.1778(7)
β (deg)	90.0130(10)	90.0540(10)	90.3720(10)	90.3240(10)
V (Å^3), Z	4560.9(3)	4560.4(2)	4536.1(2)	4600.4(2)
λ (Å)	0.710 73	0.710 73	0.710 73	0.710 73
D_c (Mg/m^3)	1.405	1.394	1.415	1.356
μ, Mo Kα (mm^{-1})	1.613	1.438	1.710	1.336
T (K)	100(2)	100(2)	100(2)	100(2)
R_1, wR_2[c]	0.0384, 0.0639	0.0437, 0.0750	0.0408, 0.0721	0.0422, 0.0734

[a] Previous work.[27] [b] Previous work.[26] [c] Structure was refined on F^2 using all reflections: $wR_2 = [\Sigma[w(F^2 - F_c^2)^2]/\Sigma[w(F^2)^2]^{1/2}$, where $w^{-1} = [\Sigma(F^2) + (aP)^2 + bP]$ and $P = [\max(F^2,0) + 2F_c^2]/3$.

2.2.2. Binary Complex Binding Studies. Association constants for Ln^{3+} to DPA^{2-} (Ln = Sm, Eu, Tb, and Dy) were determined via titration of Ln^{3+} against 10.0 nM DPA in 0.2 M sodium acetate (pH 7.4). A linear fit similar to that of the one-step equilibrium model of Jones and Vullev[22] was applied as $[Ln^{3+}] > [DPA^{2-}]$, and the binding affinity of the binary complex (K_a) was calculated using the following linear relationship:

$$\log\left(\frac{R}{C_{Ln}}\right) = \log(1 - R) + \log K_a$$
$$R = \frac{[LnDPA]_{eq}}{[LnDPA]_{eq} + [DPA]_{eq}} \quad (1)$$

where C_{Ln} is the total concentration of the lanthanide and R is the normalized integrated emission intensity (see Supporting Information for derivation). This was performed for all four lanthanides at 10, 25, 35, and 50 °C.

2.2.3. BAC Assay. Samples were prepared using solvated $Ln(DO2A)(DPA)^-$ crystals and lanthanide chloride salts in 0.2 M sodium acetate (pH 7.4), such that the concentration of $Ln(DO2A)(DPA)^-$ was 1.0 μM and the concentration of free Ln^{3+} ranged from 1.0 nM to 1.0 mM. Association constants were calculated using the Curve Fitting Tool in Matlab with a Binding Affinity by Competition (BAC) chemical equilibrium model derived previously.[26]

2.2.4. Quantum Yields. Five concentrations ranging from 5.0 to 15.0 μM were prepared for each lanthanide complex in 0.1 M Tris (pH 7.9). Absorbance measurements were made in quartz cuvettes (1 cm path length) using a Cary 50 Bio UV/visible spectrophotometer, and luminescence measurements, also in quartz, were performed using the Fluorolog-3 fluorescence spectrometer (λ_{ex} = 280 nm). All recorded absorbances were under 0.1, and all luminescence intensities were below 5×10^5 cps (counts per second), well within the linear range of both instruments. Quantum yield measurements were standardized to L-tryptophan in deionized water (18.2 MΩ-cm resistivity) at the same excitation wavelength, pH 5 ($\Phi_{ref} = 0.13 \pm 0.01$).[29] Corrections were made for the difference in refractive index between buffered H_2O (0.1 M Tris) and pure H_2O.

2.2.5. pH Dependence. For each lanthanide, samples were prepared in triplicate from 4.00 mM stock solutions of $LnCl_3$, DPA, and DO2A to contain 10.0 μM $Ln(DO2A)(DPA)^-$ in 0.1 M buffer. Five buffers were used: MES (pK_a = 6.1), MOPS (pK_a = 7.2), TAPS (pK_a = 8.4), CHES (pK_a = 9.3), and CAPS (pK_a = 10.4), with pH adjustment to within 0.1 of the pK_a value using 50% NaOH added dropwise. Emission spectra were obtained after an equilibration time of 24 h.

2.2.6. Temperature Dependence. The series of $Tb(DO2A)(DPA)^-$ cuvettes used in the BAC assay were heated or cooled to a specified temperature (eq. time of ~24 h for each temperature point) in the range 10−50 °C using a refrigerator (Marvel Scientific), incubator (VWR), or AccuBlock digital dry bath (Labnet International). The sample chamber of the Fluorolog-3, which has a cuvette holder that can be temperature-controlled, was connected to a Neslab RTE 7 Digital Plus water heater/chiller (Thermo Scientific) to maintain the desired temperature of the cuvette during scans. The temperature of each cuvette was checked prior to and following each measurement, and these values were averaged over the set of cuvettes to produce the reported temperature.

2.2.7. Cation/Anion Competition. Cuvettes were prepared with 0.10 μM $Tb(DO2A)(DPA)^-$ or $Tb(DPA)^+$ and an excess (100, 10, 1.0, or 0.10 mM) of one of the following ions: magnesium, calcium, lithium, sodium, potassium, ammonium, cesium, acetate, nitrate, fluoride, chloride, bromide, iodide, carbonate, sulfate, phosphate, and citrate. All cations were chloride salts, and all anions were sodium salts. Solution pH was adjusted to ~7 with NaOH or HCl added dropwise. Cations or anions of particular interest (calcium, phosphate, sulfate, potassium, and carbonate) were used in competition experiments against 0.1 μM $Tb(DO2A)(DPA)^-$ in 0.1 M MOPS (pH 7.5), where the concentration of the ion was varied from 1.0 nM to 0.1 M. For ion experiments where significant competition was observed, the data were fit using the Curve Fitting Tool in Matlab with a chemical equilibrium model similar to that used for the BAC assay. We consider calcium as our example to derive this model. We start with the equilibrium described in 2, which has the corresponding equilibrium expression written in 3.

$$Tb(DO2A)(DPA)^- + Ca^{2+} \overset{K_{cation}}{\rightleftharpoons} Tb(DO2A)^+ + CaDPA \quad (2)$$

$$K_{cation} = \frac{[Tb(DO2A)^+]_{eq}[CaDPA]_{eq}}{[Tb(DO2A)(DPA)^-]_{eq}[Ca^{2+}]_{eq}} \quad (3)$$

Since $K_{Tb(DO2A)} \gg K_{Ca(DO2A)}$,[30] we assume negligible formation of Ca(DO2A) or $TbDPA^+$. As $Tb(DO2A)^+$ and CaDPA form in a ratio of 1:1 from the dissociation of one $Tb(DO2A)(DPA)^-$, we obtain eq 4.

(29) Chen, R. F. *Anal. Lett.* **1967**, *1*, 35–42.

$$[\mathrm{Tb(DO2A)^+}]_{eq} = [\mathrm{CaDPA}]_{eq} \quad (4)$$

The total concentration of Tb^{3+} is expressed in eq 5, and similarly the total concentration of Ca^{2+} is given in eq 6.

$$[\mathrm{Tb^{3+}}]_{Tot} = [\mathrm{Tb(DO2A)(DPA)^-}]_{eq} + [\mathrm{Tb(DO2A)^+}]_{eq} \quad (5)$$

$$[\mathrm{Ca^{2+}}]_{Tot} = [\mathrm{Ca^{2+}}]_{eq} + [\mathrm{CaDPA}]_{eq} \quad (6)$$

Rearranging, we have eqs 7 and 8:

$$[\mathrm{Tb(DO2A)^+}]_{eq} = [\mathrm{Tb^{3+}}]_{Tot} - [\mathrm{Tb(DO2A)(DPA)^-}]_{eq} \quad (7)$$

$$[\mathrm{Ca^{2+}}]_{eq} = [\mathrm{Ca^{2+}}]_{Tot} - [\mathrm{CaDPA}]_{eq} = [\mathrm{Ca^{2+}}]_{Tot} - [\mathrm{Tb(DO2A)^+}]_{eq} \quad (8)$$

Substituting eqs 4, 7, and 8 into 3, we have expression 9.

$$K_{cation} = \frac{\{[\mathrm{Tb^{3+}}]_{Tot} - [\mathrm{Tb(DO2A)(DPA)^-}]_{eq}\}^2}{[\mathrm{Tb(DO2A)(DPA)^-}]_{eq}([\mathrm{Ca^{2+}}]_{Tot} - [\mathrm{Tb^{3+}}]_{Tot} + [\mathrm{Tb(DO2A)(DPA)^-}]_{eq})} \quad (9)$$

After some rearranging, we have

$$(1 - K_{cation})\{[\mathrm{Tb(DO2A)(DPA)^-}]_{eq}\}^2 + (K_{cation}[\mathrm{Tb^{3+}}]_{Tot} - K_{cation}[\mathrm{Ca^{2+}}]_{Tot} - 2[\mathrm{Tb^{3+}}]_{Tot})[\mathrm{Tb(DO2A)(DPA)^-}]_{eq} + \{[\mathrm{Tb^{3+}}]_{Tot}\}^2 = 0 \quad (10)$$

Solving for $[\mathrm{Tb(DO2A)(DPA)^-}]_{eq}$, we have eq 11.

$$[\mathrm{Tb(DO2A)(DPA)^-}]_{eq} = \frac{-A + \sqrt{A^2 - 4B\{[\mathrm{Tb^{3+}}]_{Tot}\}^2}}{2B} \quad (11)$$

where

$$A = (K_{cation} - 2)[\mathrm{Tb^{3+}}]_{Tot} - K_{cation}[\mathrm{Ca^{2+}}]_{Tot}$$
$$B = 1 - K_{cation}$$

In terms of intensity, we need an expression in the form of 12, as only the terbium-containing species will be observable via luminescence measurements.

$$I_{obs} = c_1 I_1 + c_2 I_2 \quad (12)$$

where

$$I_1 = \text{intensity of } [\mathrm{Tb(DO2A)(DPA)^-}]_{eq}$$
$$I_2 = \text{intensity of } [\mathrm{Tb(DO2A)^+}]_{eq}$$
$$c_1 = \frac{[\mathrm{Tb(DO2A)(DPA)^-}]_{eq}}{[\mathrm{Tb(DO2A)(DPA)^-}]_{Tot}}$$
$$c_2 = \frac{[\mathrm{Tb(DO2A)^+}]_{eq}}{[\mathrm{Tb(DO2A)(DPA)^-}]_{Tot}} = 1 - c_1$$

Substituting in eq 11, we finally end with eq 13.

$$I_{obs} = \left(\frac{[\mathrm{Tb(DO2A)(DPA)^-}]_{eq}}{[\mathrm{Tb(DO2A)(DPA)^-}]_{Tot}}\right)I_1 + \left(1 - \frac{[\mathrm{Tb(DO2A)(DPA)^-}]_{eq}}{[\mathrm{Tb(DO2A)(DPA)^-}]_{Tot}}\right)I_2$$

$$[\mathrm{Tb(DO2A)(DPA)^-}]_{eq} = \frac{-\{(10^{-7} - [\mathrm{Ca^{2+}}]_{Tot})K_{cation} - 2(10^{-7})\} + \sqrt{\{(10^{-7} - [\mathrm{Ca^{2+}}]_{Tot})K_{cation} - 2(10^{-7})\}^2 - 4(1 - K_{cation})\{[\mathrm{Tb^{3+}}]_{Tot}\}^2}}{2(1 - K_{cation})} \quad (13)$$

This equation was used in the Matlab Curve-Fit Toolbox to fit the calcium competition experiment data and calculate the competition constants.

2.2.8. Bacterial Spore Study. Approximately 100 μL of a *Bacillus atrophaeus* bacterial spore stock suspension (approximate concentration 10^9 spores/mL) was diluted to 500 μL in a sterile microcentrifuge tube with filter-sterilized deionized water (18.2 MΩ-cm resistivity). The spores were washed twice via centrifugation (16 100 rcf for 20 min), decanting the supernatant and resuspending the pellet in 500 μL of filter-sterilized deionized water. The washed spores were diluted 1:50 using filter-sterilized deionized water. The bacterial spore concentration was determined using enumeration under phase-contrast microscopy to be 3.11×10^7 ($\pm 6.11 \times 10^6$) spores/mL. The solution was then diluted to 1.00×10^5 spores/mL, and samples were prepared in quintuplicate as follows: two 2.97 mL aliquots of the spore suspension were transferred to two microwave tubes and sealed using a crimper. Ten microwave tubes, along with two sets of controls containing filter-sterilized deionized water, were autoclaved at 134 °C for 45 min to lyse the spores and effect DPA release. The solution from each tube was transferred to a cuvette, to which 30 μL of either 100 μM $TbCl_3$ or $Tb(DO2A)^+$ was added to the lysed spore suspensions and the control solutions. The excitation and emission spectra were obtained following ~30 s of thorough mixing.

3. Results and Discussion

3.1. Structural Characterization. Mass spectrometry, elemental analysis, and the crystal structures confirm formation of all four $Ln(DO2A)(DPA)^-$ ternary complexes. With the exception of $Eu(DO2A)(DPA)^-$, all of the ternary complexes crystallized in the monoclinic space group $P2_1/c$. The Eu complex crystallized in the triclinic space group $P1$. The crystal structures of all four ternary complexes are superimposable (Sm structure shown in Figure 1A, Dy structure shown in Figure S2, Supporting Information), with slight differences (<0.1 Å) appearing to follow the trend of the Ln^{3+} ionic radius (Figure 1B). The coordination geometry of the lanthanide in each structure can be described as a slightly distorted capped staggered square bipyramidal conformation, with a pseudo-C2 axis passing through the DO2A core and the lanthanide (see Figure S3, Supporting Information).

3.2. Photophysics. Absorbance, luminescence excitation (λ_{Sm} = 600 nm, λ_{Eu} = 615 nm, λ_{Tb} = 544 nm, λ_{Dy} = 574 nm), and emission (λ_{ex} = 278 nm) spectra were obtained for each ternary complex. The emission spectra all display unique band splittings that are dependent on the site symmetry of the lanthanide coordination sphere, including those of Sm^{3+} ([Xe] $4f^5$) and Dy^{3+} ([Xe] $4f^9$), which exhibit Kramers' degeneracy in low

(30) Chang, C. A.; Chen, Y. H.; Chen, H. Y.; Shieh, F. K. *J. Chem. Soc., Dalton Trans.* **1998**, 3243–3248.

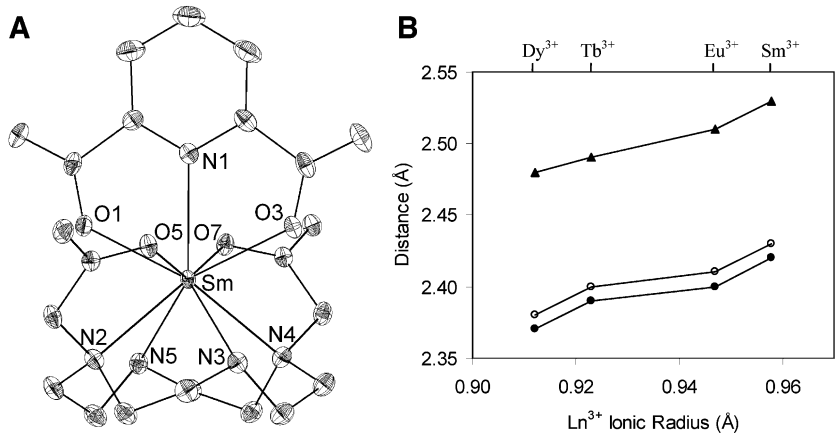

Figure 1. (A) Thermal ellipsoid plot of the Sm(DO2A)(DPA)$^-$ ternary complex with 50% probability. Hydrogens omitted for clarity. (B) Plot of Ln^{3+}---DPA interatomic distances for the four ternary complex crystal structures against Ln^{3+} ionic radius. Ln—N1 distance (▲); Ln—O1 distance (●); Ln—O3 distance (○).

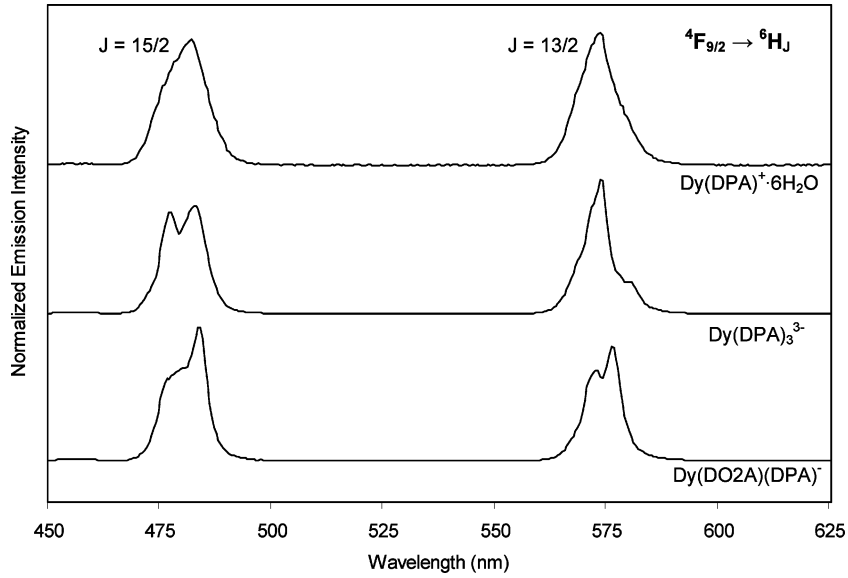

Figure 2. Emission spectra of dysprosium complexes, 10.0 μM in 0.2 M sodium acetate, pH 7.4 (λ_{ex} = 278 nm).

Table 2. Luminescence Quantum Yield Data, 0.1 M Tris Buffer, L-Trp Standard

complex	temp (°C)	pH	Φ_L ($\times 10^{-03}$)
Sm(DO2A)(DPA)$^-$	25.4 ± 0.3	7.93 ± 0.02	1.09 ± 0.03
Eu(DO2A)(DPA)$^-$	24.7 ± 0.1	7.92 ± 0.02	7.51 ± 0.03
Tb(DO2A)(DPA)$^-$	24.8 ± 0.2	7.93 ± 0.01	110 ± 2
Dy(DO2A)(DPA)$^-$	25.6 ± 0.3	7.87 ± 0.02	5.58 ± 0.07

symmetry cases.[31] For all four lanthanides this splitting is present in all observable emission peaks, regardless of hypersensitivity (i.e., the $^5D_0 \rightarrow {}^7F_2$ transition of Eu^{3+}), degeneracy of the lanthanide ground state, or whether assigned as electric dipole or magnetic dipole transitions. For example, emission spectra of the mono $Dy(DPA)^+ \cdot 6H_2O$ complex, the homoleptic $Dy(DPA)_3^{3-}$ species, and ternary Dy(DO2A)(DPA)$^-$ all exhibit very different splittings (Figure 2), and these characteristic differences can be used to visually identify the major component in solution. Emission spectra for the other three lanthanides are included in the Supporting Information.

The luminescence quantum yields for Tb complexes are greater than those of the Dy, Eu, and Sm complexes (Table 2). This is most likely due to (1) the small energy gap and corresponding strong coupling between the DPA triplet state and the terbium $^5D_4$ excited state[32,33] and (2) the absence of other terbium excited states lower in energy than the DPA triplet, which might quench emission via nonradiative decay.[34] For the case of Dy, the quantum yield is lower despite an even smaller energy gap[35] (Table 3), because the $^4I_{15/2}$ and $^4G_{11/2}$ excited states are also populated and each contributing to the loss of quantum yield via nonradiative decay.[36] The high efficiency and intensity of the Tb complex confirm our choice of this lanthanide in the $Ln(DO2A)^+$ binary complex as the optimal dipicolinate receptor site.

3.3. Lanthanide Selection. We applied a method similar to that used by Jones and Vullev to calculate the binding affinity of Ln^{3+} and DPA^{2-} (Ln = Sm, Eu, Tb, and Dy) at 25 °C. Our

(31) Görller-Walrand, C.; Binnemans, K. In *Handbook on the Physics and Chemistry of Rare Earths*; Gschneidner, J. K. A., Eyring, L., Eds.; Elsevier Science B. V.: New York, 1996; Vol. 23, pp 122−283.
(32) Arnaud, N.; Vaquer, E.; Georges, J. *Analyst* **1998**, *123*, 261–265.
(33) Latva, M.; Takalo, H.; Mukkala, V. M.; Matachescu, C.; RodriguezUbis, J. C.; Kankare, J. *J. Lumin.* **1997**, *75*, 149–169.
(34) Carnall, W. T.; Fields, P. R.; Rajnak, K. *J. Chem. Phys.* **1968**, *49*, 4447–4449.
(35) Hemmila, I.; Laitala, V. *J. Fluor.* **2005**, *15*, 529–542.
(36) Carnall, W. T.; Fields, P. R.; Rajnak, K. *J. Chem. Phys.* **1968**, *49*, 4424–4442.

Table 3. Ligand Energy Levels and Lanthanide Ion Resonance Levels Involved in the Absorbance-Energy Transfer-Emission (AETE) Mechanism of DPA-Sensitized Lanthanide Luminescence

ligand energy level (cm^{-1})		Ln^{3+} ion resonance level (cm^{-1})	
DPA Triplet	26 600[48]	Sm^{3+} $^4G_{5/2}$	17 900[36]
		Eu^{3+} $^5D_0$	17 264[49]
		Tb^{3+} $^5D_4$	20 500[34]
		Dy^{3+} $^4F_{9/2}$	21 100[36]

Table 4. Association Constants of Ln^{3+} and $Ln(DO2A)^+$ with DPA^{2-}, Calculated Using a One-Step Equilibration Model and the BAC Assay, Respectively, pH 7.5

Ln	log K_a	log K_a'
Sm	7.64 ± 0.05	8.44 ± 0.03
Eu	7.46 ± 0.02	8.39 ± 0.07[a]
Tb	7.41 ± 0.03	9.25 ± 0.13[b]
Dy	7.57 ± 0.03	8.79 ± 0.03

[a] Previous work.[26] [b] Previous work.[27]

results (Table 4) for the terbium case are in agreement with the formation constant obtained by Jones and Vullev at a similar pH.[22] Following calculation of the Ln−DPA binding affinity, the BAC assay[26] was utilized to calculate the association constant of the given $Ln(DO2A)^+$ binary complex for DPA^{2-} (Figure 3). As seen in Figure 4, the addition of the DO2A ligand enhances the binding affinity of the Ln^{3+} ion for DPA^{2-} by at least an order of magnitude. Interestingly, the binding affinity of the $Tb(DO2A)^+$ binary complex is even more effective and nearly an order of magnitude greater than the other three lanthanides. This high order of stability is maintained for extended periods of time, approaching one year or more (see Table S2, Supporting Information). The BAC assay was repeated at various temperatures for the Tb^{3+} and Eu^{3+} complexes; results indicate a nonlinear temperature dependence on the stability of the $Tb(DO2A)(DPA)^-$ complex over the range 10−50 °C, though a slight trend is observed for the Eu complex (Table 5). This is consistent with previous temperature dependence studies of europium complexes.[37]

Though others have noted that complex formation involving macrocyclic ligands can occur on the order of several hours to even days,[38−41] we have found that DPA binding is rapid at neutral to high pH provided that the $Tb(DO2A)^+$ binary complex is already formed in solution, as would be the case for a receptor site (see Figure S16, Supporting Information).

A pH dependence study was conducted over a range from 6.1 to 10.4 to determine the extent of ternary complex stability. The number of DPA molecules bound per lanthanide was calculated using the luminescence transition with the most obvious change in band splitting (i.e., the "ligand field sensitive" peak) for the three complexes $Ln(DPA)^+$, $Ln(DPA)_3^{3-}$, and $Ln(DO2A)(DPA)^-$ and solving each pH dependence emission spectrum as a best fit of a linear combination of these three profiles. The transitions used in the calculation are as follows: Tb ($^5D_4 \rightarrow {}^7F_4$, 570−600 nm), Eu ($^5D_0 \rightarrow {}^7F_4$, 675−710 nm), Dy ($^4F_{9/2} \rightarrow {}^6H_{13/2}$, 555−595 nm), Sm ($^4G_{5/2} \rightarrow {}^6H_{7/2}$, 580−625 nm). With the DO2A ligand bound, a ratio of one DPA molecule per lanthanide is maintained over the entire pH range, meaning all four lanthanide ternary complexes remained stable (Figure 5). In contrast, the $Ln(DPA)^+$ complexes began to form the tris $Ln(DPA)_3^{3-}$ species at high pH as evidenced by the Ln/DPA ratio approaching 1:3, indicating precipitation of some of the lanthanide as $Ln(OH)_3$. This result indicates that the addition of the DO2A ligand prevents precipitation of the trivalent lanthanide cation and confers additional stability to the complex.

3.4. Interferents and Detection of Bacterial Spores. A screen was performed to test the robustness of the $Tb(DO2A)^+$ receptor site in the presence of common environmental interferents. Addition of common cations and anions in excess (3 to 6 orders of magnitude) to nanomolar $Tb(DO2A)(DPA)^-$ at near neutral pH resulted in minimal emission intensity change for most ions in comparison to the $Tb(DPA)^+$ complex (see Figures S10−S13, Supporting Information). For most potential ionic interferents, the inclusion of DO2A improved luminescence intensity to some degree ($\leq 10^2$-fold) when the ion concentration was up to 6 orders of magnitude greater than the Tb−DPA concentration. Carbonate interference was only observed at concentrations 5 orders of magnitude or greater than that of Tb−DPA; in this regime, DO2A improves DPA sensing efficiency 10-fold. Citrate interferes significantly with Tb−DPA complexation; this is mitigated with the use of DO2A for concentrations up to 5 orders of magnitude greater than Tb−DPA. DO2A complexation successfully eliminates phosphate interference for concentrations up to 5 orders of magnitude greater than Tb and DPA (Figure 6).

Competition experiments were performed for selected ions (see Figure S14, Supporting Information); of those, only calcium demonstrated any significant competition with $Tb(DO2A)^+$ for DPA^{2-}, and only at $\sim 10^4$ excess (Figure 7). This was expected, as CaDPA is a stable neutral salt ($\log K_{CaDPA} = 4.05$[42]) and the mode by which most bacterial spores store the high concentration of dipicolinic acid present in the spore cortex.[14] The data were fit to a two-state chemical equilibrium model similar to that used in the BAC assay, and competition constants were calculated for Ca^{2+} competing with the $Tb(DO2A)^+$ binary complex ($\log K_{cation} = -4.36 \pm 0.23$) and the Tb^{3+} ion alone ($\log K_{cation} = -3.68 \pm 0.17$) for DPA^{2-}. The addition of the DO2A ligand improves the stability of Tb−DPA binding by a factor of 4.7 compared to the ion alone, increasing the range over which this receptor site can be used in environmental conditions.

Phosphate has been shown to severely inhibit DPA^{2-} binding to Tb^{3+} in previous studies, completely quenching Tb luminescence via an unknown mechanism even when DPA is in excess.[22,23] This was supported in the competition experiment for phosphate with $Tb(DPA)^+$; however, application of DO2A successfully mitigated phosphate interference in the binding of DPA^{2-} to Tb^{3+} by more than 3 orders of magnitude compared to Tb^{3+} alone (Figure 8).

With the superior stability and performance of the $Tb(DO2A)^+$ binary complex over Tb^{3+} alone verified experimentally, we have applied this novel DPA receptor site to the detection of actual bacterial spores. *Bacillus atrophaeus* bacterial spores have been well characterized in the literature[43−45] and

(37) Yerly, F.; Dunand, Frank A.; Tóth, É.; Figueirinha, A.; Kovács, Z.; Sherry, A. D.; Geraldes, C. F. G. C.; Merbach, A. E. *Eur. J. Inorg. Chem.* **2000**, *2000*, 1001–1006.
(38) Kumar, K.; Jin, T. Z.; Wang, X. Y.; Desreux, J. F.; Tweedle, M. F. *Inorg. Chem.* **1994**, *33*, 3823–3829.
(39) Wang, X.; Jin, T.; Comblin, V.; Lopez-Mut, A.; Merciny, E.; Desreux, J. F. *Inorg. Chem.* **1992**, *31*, 1095–1099.
(40) Brucher, E.; Laurenczy, G.; Makra, Z. S. *Inorg. Chim. Acta* **1987**, *139*, 141.
(41) Huskens, J. *Inorg. Chem.* **1997**, *36*, 1495–1503.
(42) Chung, L.; Rajan, K. S.; Merdinge, E; Grecz, N. *Biophys. J.* **1971**, *11*, 469–482.

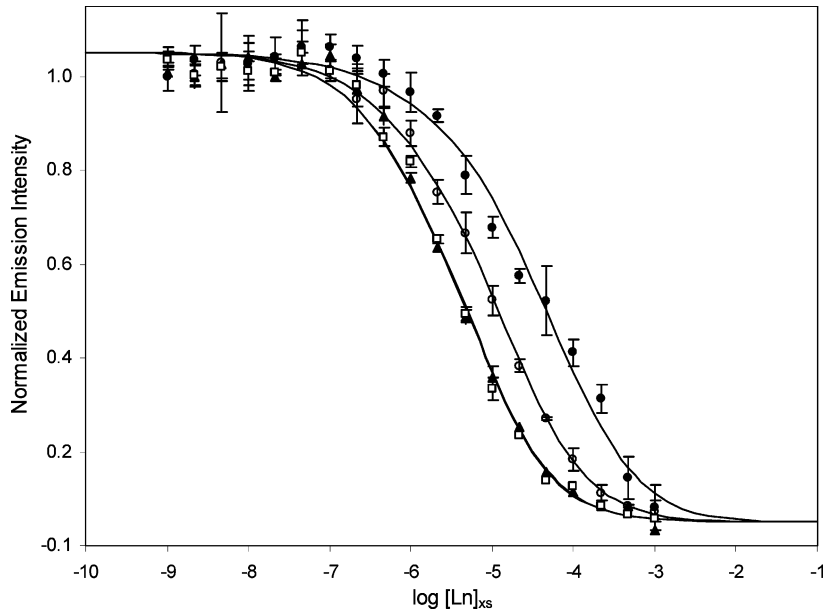

Figure 3. BAC assay applied to the four Ln(DO2A)(DPA)$^-$ ternary complexes (Ln = Sm □, Eu ▲, Tb ●, Dy ○) to determine the binding affinity of the Ln(DO2A)$^+$ binary complex for the DPA^{2-} analyte, 0.2 M sodium acetate, pH 7.5 (λ_{ex} = 278 nm).

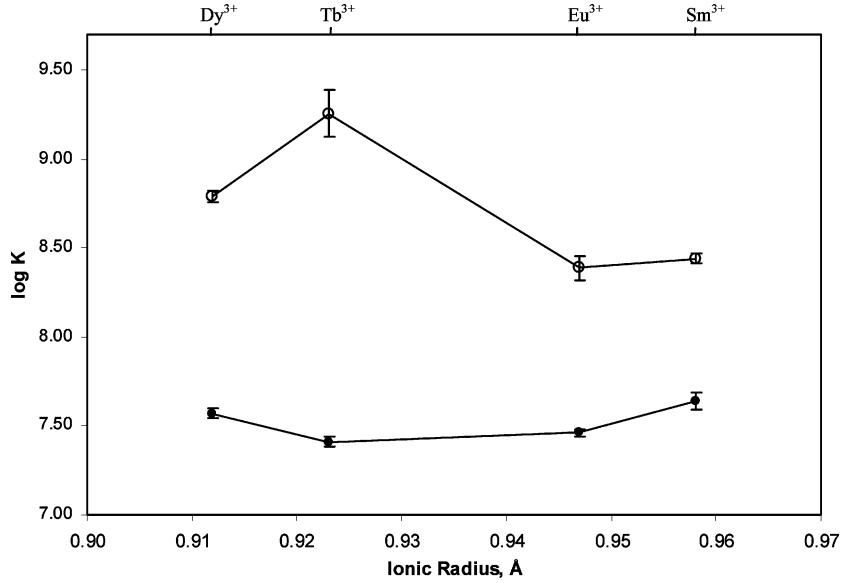

Figure 4. Association constants of Ln^{3+} (●) and Ln(DO2A)$^+$ (○) to DPA^{2-} against lanthanide ionic radius, 0.2 M sodium acetate, pH 7.5, 25 °C (λ_{ex} = 278 nm).

Table 5. Temperature Dependence of Association Constants (log K_a') of Ln(DO2A)$^+$ and DPA^{2-} Calculated Using BAC Assay

temp (°C)	Tb	Eu
10.8	9.09 ± 0.04	8.49 ± 0.01
25.0	9.25 ± 0.13[a]	8.39 ± 0.07[b]
34.8	9.00 ± 0.08	8.25 ± 0.07
50.0	8.68 ± 0.05	7.93 ± 0.03

[a] Previous work.[27] [b] Previous work.[26]

represent spores found in typical environmental samples in their relative size and DPA content.[8,47] The use of DO2A in the detection of real bacterial spores not only doubles the luminescence intensity but also improves the signal-to-noise ratio 3-fold (Figure 9). It is important to note that this result was achieved for low concentrations of bacterial spores without any sample purification (filtration to remove cell debris, extraction, pH adjustment, etc.), minimizing sample preparation while maximizing endospore detection.

(43) Fritze, D.; Pukall, R. *Int. J. Syst. Evol. Microbiol.* **2001**, *51*, 35–37.
(44) Setlow, P. *J. Appl. Microbiol.* **2006**, *101*, 514–525.
(45) Kunst, F.; Ogasawara, N.; Moszer, I.; Albertini, A. M.; Alloni, G.; Azevedo, V.; Bertero, M. G.; Bessières, P.; Bolotin, A.; Borchert, S.; Borriss, R.; Boursier, L.; Brans, A.; Braun, M.; Brignell, S. C.; Bron, S. *Nature* **1997**, *390*, 249–256.
(46) Fichtel, J.; Koster, J.; Rullkotter, J.; Sass, H. *FEMS Microbiol. Ecol.* **2007**, *61*, 522–532.
(47) Sojka, B.; Ludwig, H. *Pharm. Ind.* **1997**, *59*, 355–359.
(48) Sharma, P. K.; Van Doorn, A. R.; Staring, A. G. J. *J. Lumin.* **1994**, *62*, 219–225.
(49) Carnall, W. T.; Fields, P. R.; Rajnak, K. *J. Chem. Phys.* **1968**, *49*, 4450–4455.

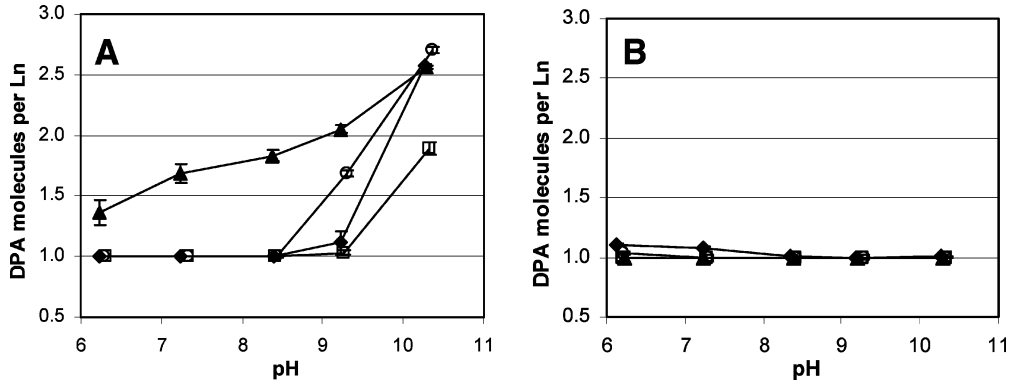

Figure 5. Number of DPA molecules bound per Ln^{3+} as a function of pH for (A) $Ln(DPA)^{+}$ and (B) $Ln(DO2A)(DPA)^{-}$ complexes (Ln = Sm □, Eu ▲, Tb ◆, Dy ○), 10.0 μM in 0.1 M buffer (λ_{ex} = 278 nm).

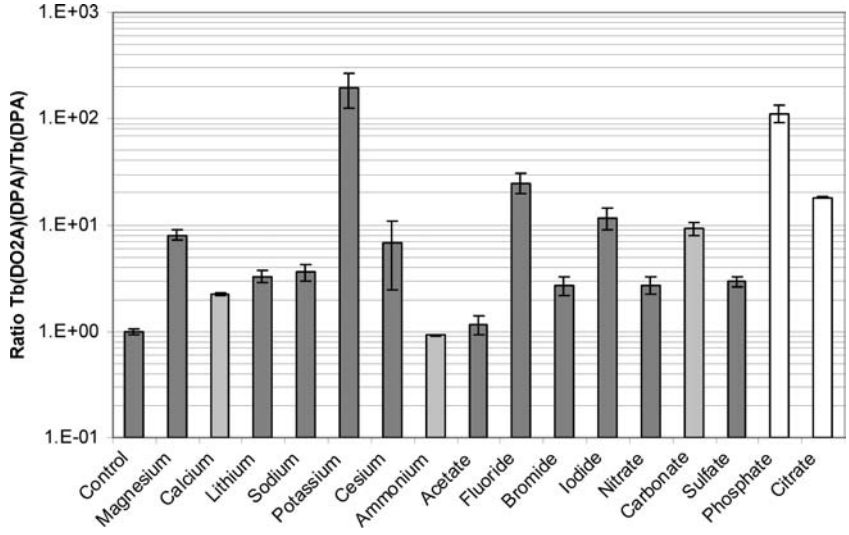

Figure 6. Ratio of emission intensity (λ_{em} = 530−560 nm, λ_{ex} = 278 nm) of 0.1 μM $Tb(DO2A)(DPA)^{-}$ complex to 0.1 μM $Tb(DPA)^{+}$ complex in the presence of 100 mM (dark gray), 10 mM (light gray), or 1 mM (white) competing ion at pH 6.6.

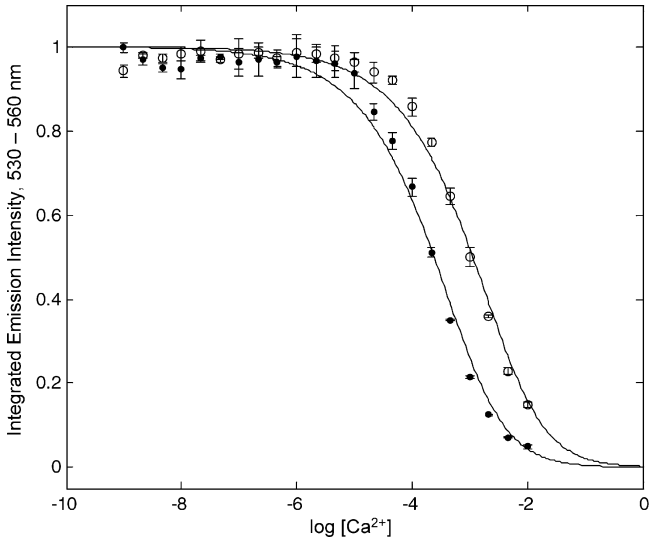

Figure 7. Cation competition experiment of 0.1 μM $Tb(DO2A)(DPA)^{-}$ (○) or $Tb(DPA)^{+}$ (●) titrated with Ca^{2+} over a concentration range from 1.0 nM to 0.1 M, pH 7.5 (0.1 M MOPS).

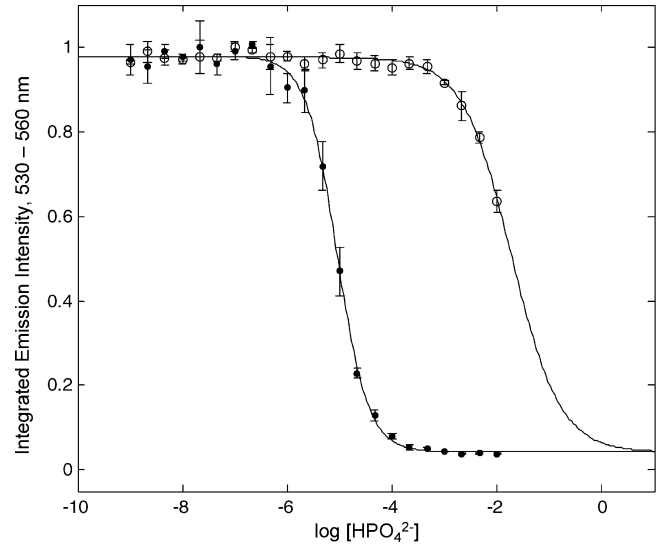

Figure 8. Anion competition experiment of 0.1 μM $Tb(DO2A)(DPA)^{-}$ (○) or $Tb(DPA)^{+}$ (●) titrated with phosphate over a concentration range from 1.0 nM to 0.1 M, pH 7.3 (0.1 M MOPS).

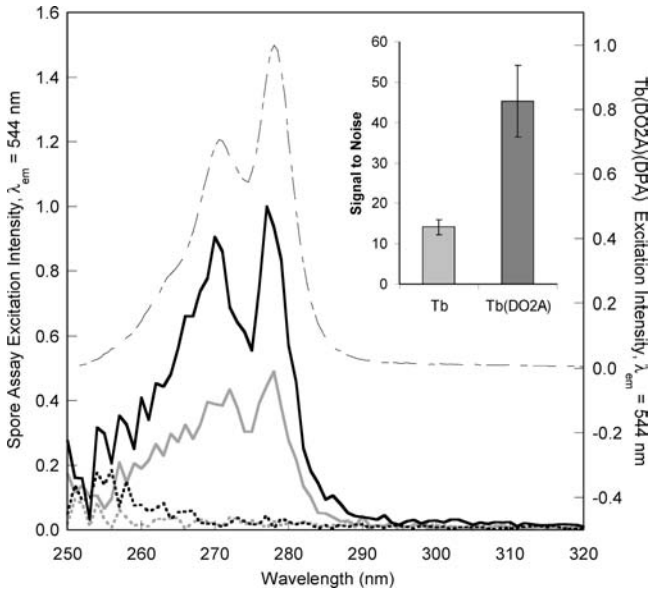

Figure 9. Excitation spectra of unfiltered samples of autoclaved *Bacillus atrophaeus* spores containing 10 μM Tb^{3+} alone (gray solid) or the $Tb(DO2A)^+$ binary complex (black solid) in filter-sterilized nanopure H_2O. Dashed offset excitation spectrum of 10 μM Tb(DO2A)(DPA) in 0.2 M sodium acetate, pH 7.4, confirms excitation profile as DPA. Concentration of bacterial spores $\sim 10^5$ spores/mL. Controls of Tb^{3+} or $Tb(DO2A)^+$ are shown in dotted gray and black, respectively. Inset: Signal-to-noise ratio of emission intensity, 530−560 nm, for Tb^{3+} (light gray) and $Tb(DO2A)^+$ (dark gray), showing a 3-fold improvement in *S/N* with the use of DO2A.

3.5. Concluding Remarks. The $Ln(DO2A)(DPA)^-$ series (Ln = Sm, Eu, Tb, and Dy) has been fully characterized. Close coupling of the DPA triplet excited state to the terbium $^5D_4$ excited state is responsible for enhanced intramolecular energy transfer in the $Tb(DO2A)(DPA)^-$ complex compared to the other three luminescent lanthanides studied and supports the observed trend in quantum yield. The application of DO2A successfully mitigates both cationic and anionic interferents of Tb−DPA luminescence, even those as notorious as phosphate. DO2A also exhibits a substantial improvement in the signal-to-noise ratio in the detection of DPA from lysed *B. atrophaeus* spores. We therefore conclude that the $Tb(DO2A)^+$ binary complex is a rapid, robust DPA receptor for the detection of bacterial spores.

Acknowledgment. The authors thank Larry Henling and Mike Day for crystallographic analysis and Kyle Lancaster for assistance with mass spectrometry. The research described in this paper was carried out at the Jet Propulsion Laboratory, California Institute of Technology, under contract with the National Aeronautic and Space Administration and was sponsored by NASA's Astrobiology and Planetary Protection Programs (A.P., J.P.K.), the Department of Homeland Security's Chemical and Biological Research & Development Program (A.P.), the National Defense Science and Engineering Graduate Fellowship Program (M.L.C.), the NASA Graduate Student Research Program (M.L.C.), the AmGen Scholars Program (D.J.L.), and the Caltech Summer Undergraduate Research Fellowship Program (D.J.L., M.J.M.). Work at the Beckman Institute was supported by the NIH, NSF, and the Arnold and Mabel Beckman Foundation (H.B.G.).

Supporting Information Available: Crystallographic data (CIF) of the $Ln(DO2A)(DPA)^-$ complexes, where Ln = Sm, Eu, Tb, or Dy; derivation of model for Ln(DPA) binding affinity; thermal ellipsoid plots of $Dy(DO2A)(DPA)^-$ ternary complex and Sm coordination geometry; normalized excitation and absorption spectra of $Ln(DO2A)(DPA)^-$ complexes; calculation of quantum yields and molar extinction coefficients for $Ln(DO2A)(DPA)^-$ complexes; K_a' values of $Tb(DO2A)(DPA)^-$ complex over time; emission spectra of various terbium, europium, and samarium complexes; emission intensity variation in $Tb(DO2A)(DPA)^+$ due to interference from common cations and anions; ion competition experiments with phosphate, sulfate, potassium, and carbonate; enthalpic and entropic components for $Tb(DO2A)(DPA)^-$ and $Eu(DO2A)(DPA)^-$; time courses of DPA binding to $Tb(DO2A)^+$ at various pH values; and calculation of signal-to-noise ratio for the bacterial spore detection study. This material is available free of charge via the Internet at http://pubs.acs.org.

JA902291V